J|A|C|S ARTICLES

Published on Web 01/29/2010

Conformational Changes of an Ion Channel Detected Through Water−Protein Interactions Using Solid-State NMR Spectroscopy

Wenbin Luo and Mei Hong*

Department of Chemistry, Iowa State University, Ames, Iowa 50011

Received November 12, 2009; E-mail: mhong@iastate.edu

Abstract: The influenza A virus M2 protein is a pH-gated and amantadine-inhibited proton channel important for the virus life cycle. Proton conduction by M2 is known to involve water; however direct experimental evidence of M2-water interaction is scarce. Using ^{1}H spin diffusion solid-state NMR, we have now determined the water accessibility of the M2 transmembrane domain (M2-TM) in virus-envelope-mimetic lipid membranes and its changes with environment. Site-specific water−protein magnetization transfer indicates that, in the absence of amantadine, the initial spin diffusion rate mainly depends on the radial position of the residues from the pore: pore-lining residues along the helix have similarly high water accessibilities compared to lipid-facing residues. Upon drug binding, the spin diffusion rates become much slower for Gly_{34} in the middle of the helix than for the N-terminal residues, indicating that amantadine is bound to the pore lumen between Gly_{34} and Val_{27}. Water−protein spin diffusion buildup curves indicate that spin diffusion is the fastest in the low-pH open state, slower in the high-pH closed state, and the slowest in the high-pH amantadine-bound state. Simulations of the buildup curves using a 3D lattice model yielded quantitative values of the water-accessible surface area and its changes by pH and drug binding. These data provide direct experimental evidence of the pH-induced change of the pore size and the drug-induced dehydration of the pore. This study demonstrates the capability of ^{1}H spin diffusion NMR for elucidating water interactions with ion channels, water pores, and proton pumps and for probing membrane protein conformational changes that involve significant changes of water-accessible surface areas.

Introduction

Water is essential for the folding and functions of ion channels,[1,2] water pores,[3] and proton pumps in biological membranes[4,5] and is important for the solvation of charged residues in lipid bilayers.[6−8] Elucidating the interaction of water with membrane proteins and water dynamics in the low-dielectric core of the lipid membrane[9] is thus of fundamental interest. The influenza A M2 protein forms a pH-gated proton channel in the virus envelope that is important for the virus lifecycle.[10−12] Acidification of the virus particle triggers the release of the viral RNA into the infected cell, initiating virus replication. The M2 channel activity is mediated by water molecules and by the action of a key residue, His_{37},[13] and is inhibited by amantadine and rimantadine.[14] Recent high-resolution structural studies of the M2 protein by X-ray crystallography[15] and NMR spectroscopy[16−18] provided a wealth of information about the global and site-specific conformational features important for proton conduction. However, direct experimental evidence about how water interacts with the M2 protein under different pH and drug-binding conditions is still scarce. Most proposals for the mechanism of proton conduction so far came from molecular dynamics (MD) simulations.[19−21]

Solid-state NMR (SSNMR) spectroscopy provides a unique and powerful tool for studying water−protein interactions

(1) Swartz, K. J. *Nature* **2008**, *456*, 891–897.
(2) Swanson, J. M.; Maupin, C. M.; Chen, H.; Petersen, M. K.; Xu, J.; Wu, Y.; Voth, G. A. *J. Phys. Chem. B* **2007**, *111*, 4300–4314.
(3) Fu, D.; Lu, M. *Mol. Membr. Biol.* **2007**, *24*, 366–374.
(4) Brzezinski, P.; Gennis, R. B. *J. Bioenerg. Biomembr.* **2008**, *40*, 521–531.
(5) Lanyi, J. K. *Biochim. Biophys. Acta* **2006**, *1757*, 1012–1018.
(6) Freites, J. A.; Tobias, D. J.; von Heijne, G.; White, S. H. *Proc. Natl. Acad. Sci. U.S.A.* **2005**, *102*, 15059–15064.
(7) Dorairaj, S.; Allen, T. W. *Proc. Natl. Acad. Sci. U.S.A.* **2007**, *104*, 4943–4948.
(8) MacCallum, J. L.; Bennett, W. F.; Tieleman, D. P. *Biophys. J.* **2008**, *94*, 3393–3404.
(9) Rasaiah, J. C.; Garde, S.; Hummer, G. *Annu. Rev. Phys. Chem.* **2008**, *59*, 713–740.
(10) Pinto, L. H.; Holsinger, L. J.; Lamb, R. A. *Cell* **1992**, *69*, 517–28.
(11) Pinto, L. H.; Lamb, R. A. *J. Biol. Chem.* **2006**, *281*, 8997–9000.
(12) Cady, S. D.; Luo, W. B.; Hu, F.; Hong, M. *Biochemistry* **2009**, *48*, 7356–7364.
(13) Wang, C.; Lamb, R. A.; Pinto, L. H. *Biophys. J.* **1995**, *69*, 1363–1371.
(14) Wang, C.; Takeuchi, K.; Pinto, L. H.; Lamb, R. A. *J. Virol.* **1993**, *67*, 5585–5594.
(15) Stouffer, A. L.; Acharya, R.; Salom, D.; Levine, A. S.; Di Costanzo, L.; Soto, C. S.; Tereshko, V.; Nanda, V.; Stayrook, S.; DeGrado, W. F. *Nature* **2008**, *451*, 596–599.
(16) Hu, J.; Fu, R.; Nishimura, K.; Zhang, L.; Zhou, H. X.; Busath, D. D.; Vijayvergiya, V.; Cross, T. A. *Proc. Natl. Acad. Sci. U.S.A.* **2006**, *103*, 6865–6870.
(17) Luo, W.; Mani, R.; Hong, M. *J. Phys. Chem.* **2007**, *111*, 10825–10832.
(18) Schnell, J. R.; Chou, J. J. *Nature* **2008**, *451*, 591–595.
(19) Smondyrev, A. M.; Voth, G. A. *Biophys. J.* **2002**, *83*, 1987–1996.
(20) Yi, M.; Cross, T. A.; Zhou, H. X. *J. Phys. Chem. B* **2008**, *112*, 7977–7979.
(21) Khurana, E.; Dal Peraro, M.; DeVane, R.; Vemparala, S.; DeGrado, W. F.; Klein, M. L. *Proc. Natl. Acad. Sci. U.S.A.* **2009**, *106*, 1069–1074.

10.1021/ja9096219

directly in native lipid bilayers.[22,23] Correlation of water−protein $^{1}H-^{13}C$ signals after dipolar-driven ^{1}H spin diffusion gives detailed information about the proximity of protein residues to water. The rate of ^{1}H spin diffusion was initially used to determine the global topology of membrane proteins[24] and was recently shown to also give information about the water−protein surface area.[25]

In this study, we use water-to-protein ^{1}H spin diffusion NMR to investigate the water accessibilities and water dynamics of the M2 transmembrane peptide (M2-TM) in virus-envelope-mimetic lipid bilayers.[26] We demonstrate that the spin diffusion buildup rates are site specific and differ between lipid-facing and pore-lining residues in the absence of drug; thus the source of water magnetization is primarily the pore water. We show that a 3D lattice model can be used to simulate the spin diffusion buildup and quantify the water-exposed protein surface area. The result indicates a close correlation between the water accessibility and the function of the M2 proton channel.

Materials and Methods

Membrane Protein Samples. M2(22−46) of the Udorn strain (SSDPLVVAASIIGILHLIL WILDRL) was synthesized and purified by PrimmBiotech (Cambridge, MA). Two peptide samples containing uniformly ^{13}C, ^{15}N-labeled residues at Leu_{26}, Val_{27}, Ala_{29}, Gly_{34}, and Ile_{35} were synthesized. The samples used for low- and high-pH experiments without amantadine contained labeled Leu_{26}, Val_{27}, Ala_{29}, and Gly_{34}, while the peptide used for the high-pH drug-bound experiments contained labeled Leu_{26}, Ala_{29}, Gly_{34}, and Ile_{35}. The peptide was reconstituted by detergent dialysis[27] into a lipid mixture mimicking the virus-envelope-lipid composition.[26] The mixture contains egg sphingomyelin (SPM), DPPC, DPPE, and cholesterol at the molar ratio of 28%:21%:21%:30%. SPM was dissolved in a chloroform/methanol (5: 1) solution before mixing with the other lipids. The lipid mixture was lyophilized, suspended in a buffer of desired pH, vortexed, and freeze−thawed several times to form large unilamellar vesicles. A phosphate buffer containing 10 mM Na_2HPO_4/NaH_2PO_4, 1 mM EDTA, and 0.1 mM NaN_3 was used for the pH 7.5 samples, and a citrate buffer with 10 mM citric acid/sodium citrate, 1 mM EDTA, and 0.1 mM NaN_3 was used for the pH 4.5 sample. The molar ratio of M2 monomer to lipids (not counting cholesterol) was 1:15. The proteoliposome suspensions were centrifuged at 150 000 *g* to obtain 40% hydrated pellets. Photometric assays showed >95% binding of M2-TM to the membrane. For the amantadine-bound sample, amantadine hydrochloride in the pH 7.5 buffer was directly titrated to the pellet to reach an M2 monomer/amantadine (Amt) molar ratio of 1:2.

Solid-State NMR Experiments. NMR experiments were carried out on wide-bore Bruker NMR spectrometers at 14.1 and 9.4 T using 4 mm magic-angle spinning (MAS) probes. Typical radio frequency field strengths were 50 kHz for ^{13}C and ^{31}P and 60−70 kHz for ^{1}H. ^{13}C and ^{31}P chemical shifts were referenced to the α-Gly ^{13}CO signal at 176.49 ppm on the TMS scale and the hydroxyapatite ^{31}P signal at +2.73 ppm on the phosphoric acid scale, respectively. ^{1}H chemical shifts were internally referenced to the lipid Cγ signal at 3.26 ppm on the TMS scale.

All 1D and 2D ^{1}H spin diffusion experiments with ^{13}C or ^{31}P detection[28] were conducted at 293 K, where water is mobile but the protein is immobilized.[26] The 2D $^{1}H-^{13}C$ and $^{1}H-^{31}P$ correlation experiments used a ^{1}H T_2 filter of 2 and 0.8 ms, respectively, to suppress the ^{1}H magnetization of the rigid components. Spin diffusion mixing times (t_m) were 64 ms for the 2D $^{1}H-^{31}P$ experiments and 4 to 100 ms for the 2D $^{1}H-^{13}C$ experiments. ^{13}C double-quantum (DQ) filtered 1D spin diffusion experiments, which removed the lipid ^{13}C signals, used the SPC-5 sequence[29] to create the DQ coherence and a ^{1}H T_2 filter of 2 ms. Most spin diffusion spectra were measured under 5 kHz MAS.

Water−protein spin diffusion intensity as a function of the square root of t_m (eq 1) was plotted after correcting for water T_1 relaxation. The water ^{1}H T_1 was measured using the standard inversion recovery sequence. Water ^{1}H T_2 relaxation times were measured using a Hahn-echo experiment and detected through the protein ^{13}C signals.

Theoretical Frameworks for Determining Water−Protein Surface Areas from ^{1}H Spin Diffusion. The analytical theory for determining the water−protein surface areas from spin diffusion NMR has been well developed for heterogeneous polymers.[30] The protein ^{1}H magnetization I_P increases with the spin diffusion mixing time t_m due to relayed magnetization transfer from water according to

$$\frac{I_P(t_m)}{I_P(\infty)} \approx \sqrt{\frac{D_{eff}}{\pi}}\frac{S_{WP}}{V_P}\sqrt{t_m} \tag{1}$$

where D_{eff} is the effective spin diffusion coefficient of the entire system, S_{WP} is the water−protein surface area, and V_P is the protein volume. Equation 1 indicates that the water-to-protein spin diffusion buildup with time reports S_{WP}. The time t_m^s for the protein to reach equilibrium intensity $I_P(\infty)$, which can be extracted from the initial slope of the buildup curve, is inversely proportional to S_{WP}:

$$\sqrt{t_m^s} = \sqrt{\frac{\pi}{D_{eff}}}\frac{V_P}{S_{WP}} \tag{2}$$

Although this analytical approach gives useful insights into the relation between spin diffusion buildup and the water−protein surface area, it is only semiquantitative and does not capture high-resolution structural details of the protein. Simplifying assumptions about the protein three-dimensional shape, the average diffusivity of the ternary water−protein−lipid system and the volume fraction of water (see below) have been made to arrive at eq 1.[30] To determine the water accessibilities of M2-TM under more realistic conditions of heterogeneous diffusion coefficients and a decidedly uneven surface, we also calculated the ^{1}H spin diffusion buildup curves numerically using a three-dimensional lattice model.[25,30] The lattice is a low-resolution model of the M2 helical bundle in a 44-Å thick lipid bilayer representing the viral membrane. Cubes with a 2-Å side (d) were used to define the positions of water, lipids, the protein, the water−protein interface, and amantadine. The time-dependent ^{1}H magnetization at any lattice point, $M_{x,y,z}(t_m)$, was calculated in MATLAB as

$$M_{x,y,z}(t_m + \Delta t_m) = M_{x,y,z}(t_m) + \sum_{i=W,P}\frac{D_{ij}\Delta t_m}{d^2}[M_i(t_m) - M_{x,y,z}(t_m)] \tag{3}$$

$M_{x,y,z}(t_m)$ exchanges with the magnetization of its six neighbors at a rate determined by the spin diffusion coefficient D_{ij}. Previous

(22) Hong, M. *Structure* **2006**, *14*, 1731–1740.
(23) Hong, M. *Acc. Chem. Res.* **2006**, *39*, 176–183.
(24) Kumashiro, K. K.; Schmidt-Rohr, K.; Murphy, O. J.; Ouellette, K. L.; Cramer, W. A.; Thompson, L. K. *J. Am. Chem. Soc.* **1998**, *120*, 5043–5051.
(25) Ader, C.; Schneider, R.; Seidel, K.; Etzkorn, M.; Becker, S.; Baldus, M. *J. Am. Chem. Soc.* **2009**, *131*, 170–176.
(26) Luo, W.; Cady, S. D.; Hong, M. *Biochemistry* **2009**, *48*, 6361–6368.
(27) Cady, S. D.; Mishanina, T. V.; Hong, M. *J. Mol. Biol.* **2009**, *385*, 1127–1141.
(28) Huster, D.; Yao, X. L.; Hong, M. *J. Am. Chem. Soc.* **2002**, *124*, 874–883.
(29) Hohwy, M.; Jakobsen, H. J.; Eden, M.; Levitt, M. H.; Nielsen, N. C. *J. Chem. Phys.* **1998**, *108*, 2686–2694.
(30) Schmidt-Rohr, K.; Spiess, H. W. *Multidimensional Solid-State NMR and Polymers*; Academic Press: San Diego, 1994.

measurements have established a high water D_{WW} of 3 nm^2/ms, which reflects the fast physical diffusion of water. The water translation diffusion coefficient is ~2 μm^2/ms in bulk and only 2−3-fold slower in confined environments such as ion channels;[19] thus water diffuses over a distance of micrometers in 1 ms. Thus, for the nanometer-thick lipid bilayer, water is fully exchanged between the membrane surface and the channel within milliseconds as long as the water pathway is continuous. For the protein, a spin diffusion coefficient D_{PP} of 0.3 nm^2/ms was used based on measurements of rigid organic polymers.[24,28,31,32] For the water−protein interface, we used a D_{WP} of 0.008 nm^2/ms,[25] which is lower than D_{PP} and D_{WW} due to the inefficiency of spin diffusion across the intermolecular interface. This D_{WP} value falls within the range of 0.0013−0.008 nm^2/ms used before for experiments at ambient temperatures.[25,28,33] The 5-fold variation reflects the different viscosities of the lipid membranes due to the different lipid compositions and phase transition temperatures. The indirect pathway of water spin diffusion to lipids and then to the protein was neglected in the simulation due to the lack of lipid ^{1}H−protein ^{13}C cross peaks in the 2D ^{13}C−^{1}H spectra within the mixing times used, which indicates inefficient spin diffusion from the lipid to the protein.[25]

The water magnetization of each cube was kept at 1 throughout the simulation, which represents the limit of the large water reservoir. The protein magnetization was read out in 100 steps from time 0 to 625 ms to obtain the time-dependent intensity buildup curve.

Result and Discussion

Differential Water Accessibilities of M2-TM under Different pH and Drug Binding Conditions. We investigated the M2-water contact by measuring the protein ^{13}C signals that originated from water by ^{1}H spin diffusion. Using a 2D ^{1}H−^{13}C correlation experiment with a ^{1}H T_2 filter (2 ms) and no ^{1}H homonuclear decoupling during the evolution period, we removed all ^{1}H magnetization of the rigid protein;[26] thus the protein ^{13}C signals must have originated from the mobile water or lipids. The identity of the ^{1}H magnetization source was also directly verified by the ^{1}H chemical shifts in the 2D spectra. The use of a lipid mixture mimicking the virus-envelope membrane composition was essential for obtaining high-sensitivity spectra of M2-TM at physiological temperature, since the peptide undergoes intermediate-time scale motions in simple phosphocholine bilayers that severely broaden the NMR spectra.[34,35] The M2-TM reconstituted into the cholesterol-rich viral membrane is completely tetramerized, as shown by ^{19}F NMR spin counting experiments[36] and by thiol disulfide equilibria measurements that found increasing tetramerization from micelles to lipid bilayers and from thin phosphocholine bilayers to thick cholesterol-containing phosphocholine bilayers.[37] The five labeled residues represent different proximities to water: the N-terminal Leu_{26}, Val_{27}, Ala_{29} are closer to the bilayer surface water (1.0−1.5 nm) while Gly_{34} and Ile_{35} are far from the surface water (~2.2 nm).[38,39] On the other hand, Val_{27} and Gly_{34} line the channel pore while Ala_{29} faces the lipids (Figure 1d). Thus, the labeled residues allow us to examine whether spin diffusion primarily depends on the residue proximity to the bilayer-surface water or proximity to the pore water.

Figure 1 compares the 2D ^{1}H−^{13}C spectra of M2-TM under different pH and drug binding conditions. Spectra measured with a short mixing time of 4 ms were compared to those of 100 ms to qualitatively deduce the water accessibilities of the residues. To avoid comparing side chains with different segmental dynamics and thus different diffusion coefficients, we mainly focused on the Cα sites. At pH 4.5, the water cross peak intensities at 4 ms relative to 100 ms are similar between the N-terminal residues (Leu_{26} and Val_{27}) and the middle residue Gly_{34}. Since Gly_{34} is significantly deeper in the membrane, this similarity indicates that there is a continuous water pathway in the pore from the N-terminus to the center of the helical bundle, which gives pore-facing Val_{27} and Gly_{34} similar water accessibilities. In comparison, the water cross peak of the lipid-facing Ala_{29} at 4 ms is weaker than that of the other residues, indicating that the experiment is sensitive to the water accessibility difference between lipid-facing residues and pore-lining residues and that the radial distance to the pore water is the main determining factor for the water cross peak intensity at short mixing times.

At pH 7.5, the main features of the pH 4.5 spectrum is preserved, but now the Gly_{34} peak is slightly lower than the N-terminal residues at 4 ms (Figure 1b), suggesting that the amount of water in the middle of the pore is less than that at pH 4.5.

When the protein is complexed to amantadine, the relative intensities of Gly_{34} and Ile_{35} peaks at 4 ms are significantly weaker than the relative intensities of Leu_{26} and Ala_{29} peaks (Figure 1c). Thus, in the presence of drug, the N-terminus has substantially higher water accessibilities than the middle segment of the protein, suggesting that amantadine interrupts the water pathway between Ala_{29} and Gly_{34}.

The full 2D ^{1}H−^{13}C spectra do not show lipid ^{1}H−protein ^{13}C cross peaks within the mixing times of interest (<225 ms) (Figure S1). Thus, a 1D version of the 2D experiment is sufficient for extracting the water−protein buildup rates. The shorter experiments allow more mixing times to be measured so that quantitative buildup curves can be obtained. To suppress the ^{13}C signals of unlabeled lipids and cholesterol in the 1D spectra, we added a ^{13}C DQ filter. Figure 2 and Figure S2 show representative 1D ^{13}C DQ spectra and the resulting buildup curves for the three states. For all sites studied, the intensity buildup is the fastest at pH 4.5, moderately slower at pH 7.5, and more substantially slower upon amantadine binding. This trend is the most pronounced for Gly_{34}, whose buildup rate in the drug-bound state is clearly slower than that for the N-terminal residues (Figure 2e), confirming that water accessibility is lower in the middle of the TM helices than at the N-terminus in the amantadine-bound state. Quantifying the buildup rates using the initial slopes yielded t_m^s values, which are inversely related to the water-accessible surface area (Figure S3). Increasing the pH from 4.5 to 7.5 increased the average t_m^s by 20% while amantadine binding increased t_m^s by 56% compared to the open state (Table S1).

(31) Clauss, J.; Schmidt-Rohr, K.; Spiess, H. W. *Acta Polym.* **1993**, *44*, 1–17.
(32) Gallagher, G. J.; Hong, M.; Thompson, L. K. *Biochemistry* **2004**, *43*, 7899–7906.
(33) Mani, R.; Cady, S. D.; Tang, M.; Waring, A. J.; Lehrer, R. I.; Hong, M. *Proc. Natl. Acad. Sci. U.S.A.* **2006**, *103*, 16242–16247.
(34) Cady, S. D.; Goodman, C.; Tatko, C. D.; DeGrado, W. F.; Hong, M. *J. Am. Chem. Soc.* **2007**, *129*, 5719–5729.
(35) Cady, S. D.; Hong, M. *J. Biomol. NMR* **2009**, *45*, 185–196.
(36) Luo, W.; Hong, M. *J. Am. Chem. Soc.* **2006**, *128*, 7242–7251.
(37) Cristian, L.; Lear, J. D.; DeGrado, W. F. *Proc. Natl. Acad. Sci. U.S.A.* **2003**, *100*, 14772–7.
(38) Cady, S. D.; Schmidt-Rohr, K.; Wang, J.; Soto, C. S.; DeGrado, W. F.; Hong, M. *Nature* **2010**, in press.
(39) Niemela, P. S.; Hyvonen, M. T.; Vattulainen, I. *Biochim. Biophys. Acta* **2009**, *1788*, 122–135.

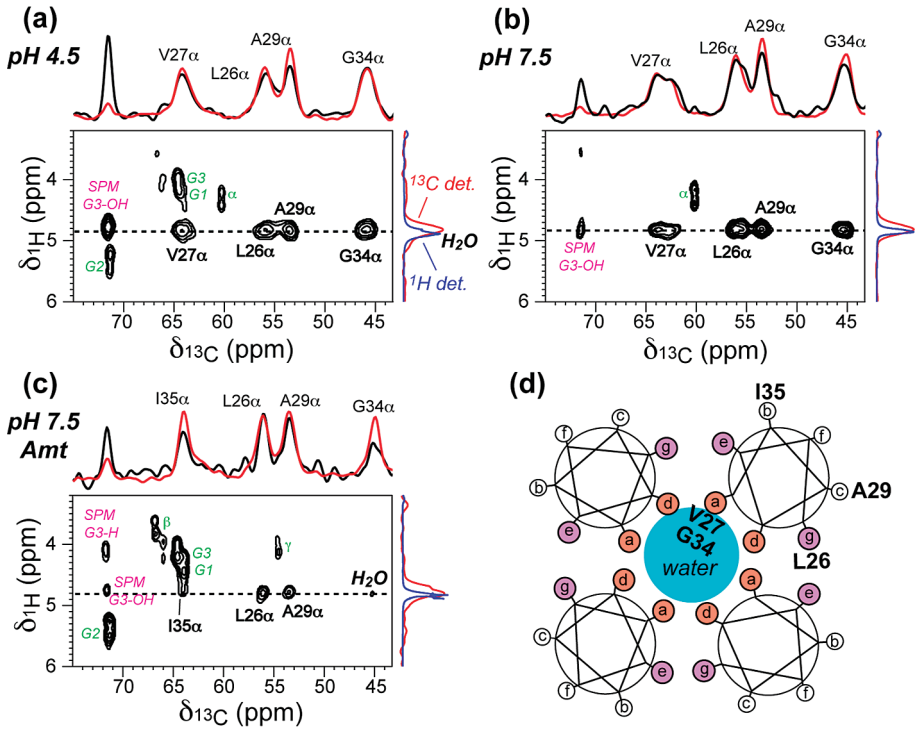

Figure 1. 2D $^{13}C-^{1}H$ correlation spectra of M2-TM in virus-envelope-mimetic lipid membranes at 293 K. A ^{1}H T_2 filter time of 2 ms and a spin diffusion mixing time of 4 ms were used. (a) pH 4.5. (b) pH 7.5. (c) pH 7.5 with amantadine. Assignments for intermolecular water−protein cross peaks (black) as well as intramolecular phospholipid peaks (green) and sphingomyelin (SPM) peaks (magenta) are indicated. The water ^{1}H cross section is shown at the top (black), superimposed with the water cross section from the 100 ms 2D spectra (red). The G34 Cα cross section at 100 ms is shown on the right (red), superimposed with the ^{1}H 1D spectra (blue) to indicate the small upfield shift of the membrane-associated water from the bulk water. (d) Schematic of the M2-TM tetrameric helical bundle, where the approximate radial positions of the labeled residues are indicated.

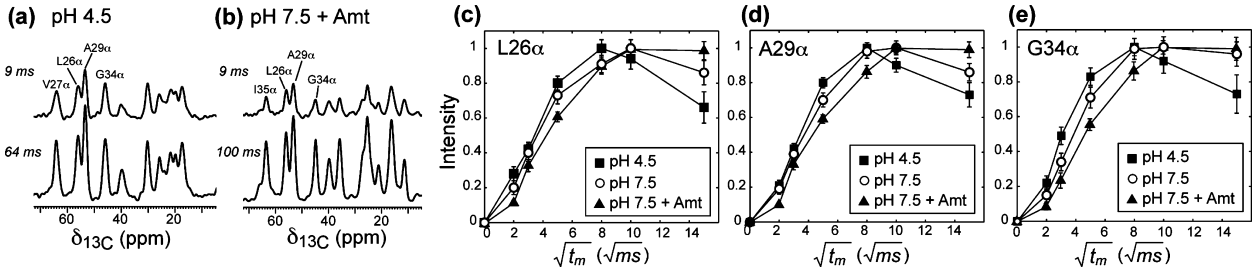

Figure 2. Water-to-M2 ^{1}H spin diffusion buildup curves from 1D ^{13}C DQ experiments. (a) Representative ^{13}C DQ filtered spectra at pH 4.5. (b) Representative ^{13}C DQ filtered spectra at pH 7.5 in the presence of amantadine. (c−e) Buildup curves of several Cα sites at pH 4.5 (■), pH 7.5 (○), and pH 7.5 with bound amantadine (▲) after correcting for water ^{1}H T_1. (c) Leu_{26}. (d) Ala_{29}. (e) Gly_{34}.

To examine whether the slower spin diffusion of the amantadine-bound M2-TM may be due to the lower water content of the sample instead of obstruction of the pore, we measured the 1D ^{1}H spectra and 2D $^{1}H-^{31}P$ correlation spectra of the three samples. The 1D ^{1}H spectra report the total water content of each sample, including both membrane-associated water and bulk water, while the 2D $^{1}H-^{31}P$ correlation spectra report the amount of interbilayer water in the multilamellar vesicles. Figure 3 shows that the total water intensity of each sample, normalized to the lipid Hγ intensity, increases in the order of pH 4.5 < pH 7.5 < pH 7.5 with amantadine. 2D $^{1}H-^{31}P$ correlation spectra further indicate that the drug-bound sample has the highest amount of membrane-associated water, since the ^{31}P-correlated water intensity is the highest for the drug-bound sample (Figure 3). Thus, the slow water-to-Gly_{34} spin diffusion in the amantadine-bound sample, despite the presence of large amounts of water on the membrane surface, must be attributed to obstruction of the water pathway in the channel.

Since the amantadine-bound sample contains 8-fold more drug than M2-TM channels, and the stoichiometry of M2 inhibition is one amantadine per channel,[14] there is significant excess drug in the lipid bilayer. At the protein/lipid molar ratio of 1:15, the amphiphilic amantadine constitutes 13 mol % of the lipid bilayer. A recent NMR relaxation analysis of the effects of amantadine on the dynamics of M2-TM and lipids[35] found that excess amantadine increases the membrane viscosity. This viscosity increase may indirectly affect water−protein spin diffusion by siphoning more water ^{1}H magnetization to the lipids due to higher diffusion coefficients of the lipids. As a result, the protein intensity at long mixing times would be lower than if the lipid diffusion coefficients were unchanged. Thus, the 100 ms protein intensity may be moderately reduced compared to the apo samples. This indirect effect most likely accounted for the smaller increase of the Ala_{29} intensity from 4 to 100 ms in the drug-bound spectrum compared to the apo spectra (Figure 1). It also strengthens the conclusion that

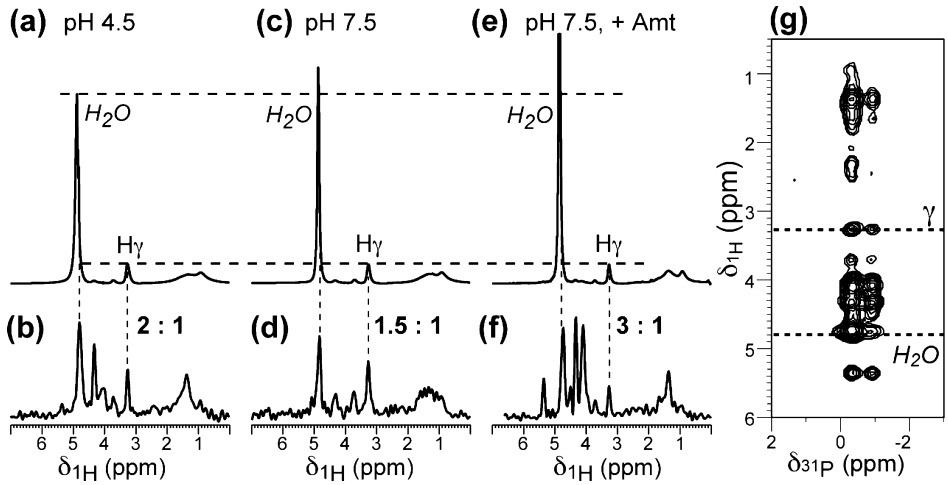

Figure 3. 1D ^{1}H direct-polarization (DP) spectra and ^{31}P-detected ^{1}H spectra extracted from 2D ^{31}P−^{1}H correlation spectra of membrane-bound M2-TM. (a, c, e) 1D ^{1}H spectra showing the full water peak. (b, d, f) Projection of the ^{1}H cross sections of the 2D ^{31}P−^{1}H spectra with 64 ms spin diffusion. (a, b) pH 4.5. (c, d) pH 7.5. (e, f) pH 7.5 with amantadine. (g) A representative 2D ^{31}P−^{1}H spectrum for the pH 7.5 sample with amantadine.

the water pathway is interrupted by amantadine: if no excess drug was present in the membrane, the intensities of Gly_{34} and Ile_{35} at short mixing times would have been even lower compared to the equilibrium intensity at long mixing times.

To assess whether the water diffusion coefficient may be affected by pH and drug binding in a way that causes the observed changes in the protein buildup curves, we measured the water-to-lipid CH_2 spin diffusion as a function of mixing time. The result shows that water−lipid spin diffusion is slower at low pH and is similar at high pH with or without the drug (Figure S5), which is opposite to the trend of the water−protein spin diffusion. Therefore, the water−protein spin diffusion changes with pH and drug binding are caused by changing water accessibilities of the protein, despite small counterdirectional changes of water and lipid diffusion rates.

Comparison of the 2D correlation spectra and the 1D ^{1}H spectra indicates that the protein- and lipid-correlated water signal resonates at a ^{1}H chemical shift of 4.73−4.83 ppm, which is ∼0.1 ppm lower than the bulk water chemical shift of 4.80−4.93 ppm (Figures 1, 3). Thus, the ^{31}P-correlated interbilayer water and the protein ^{13}C-correlated pore water have detectably different physical properties from those of the bulk water outside the multilamellar vesicles. This difference is expected due to the confinement of the membrane-associated water. On the other hand, the interbilayer water and pore water, which are within nanometers of each other, are fully averaged on the millisecond time scale due to the fast water translational diffusion; thus their chemical shifts should be indistinguishable. Indeed, the ^{13}C-detected and ^{31}P-detected water chemical shifts are identical within experimental uncertainty (Figures S1, S4).

The ability to selectively detect the pore and interbilayer water but not bulk water allowed us to probe the dynamics of protein-associated water through ^{1}H T_2 relaxation times. Water molecules in the fast motional limit should exhibit long T_2 relaxation times that increase with increasing temperature. Figure 4 shows the protein-^{13}C detected water ^{1}H T_2 at low and high pH without amantadine. The T_2 increases with temperature between 253 and 313 K for both samples, indicating fast reorientations of the water molecules, but the low-pH state has longer water T_2's than the high-pH state. Thus, water is more dynamic at low pH, again consistent with a larger pore in the open state.

Water-M2 Surface Areas from 3D Lattice Simulations. To obtain more quantitative information about how pH and

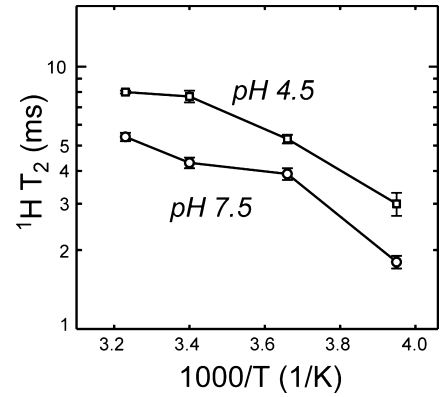

Figure 4. ^{1}H T_2 of interbilayer and channel water as a function of temperature, detected through protein ^{13}C signals after 100 ms spin diffusion. (□) pH 4.5. (○) pH 7.5. Error bars are indicated.

amantadine change the protein−water surface area, we calculated the water−protein ^{1}H spin diffusion buildup curves using a 3D lattice model, where stepwise magnetization transfer among the lattice points simulates spin diffusion in real space. In the simulation, a 44-Å thick lipid bilayer[39,40] was constructed from 2-Å sized cubes, in which the four-helix bundle was represented by appropriate numbers of cubes in each plane so that the helices were tilted by ∼25° from the bilayer normal (Figures S6−S8). This tilt angle was extrapolated from the measured M2-TM orientations in bilayers of varying thicknesses, including DLPC, DMPC, and POPC bilayers.[34,41−43] Additionally, amantadine causes a helix kink at Gly_{34}[42] with a smaller tilt angle for the C-terminal segment; thus we adjusted the protein cube positions for the amantadine-bound state to create a less tilted C-terminal segment. The total volume of the protein was kept constant at ∼12.7 nm^3 (Table 1) based on an average

(40) Duong-Ly, K. C.; Nanda, V.; DeGrado, W. F.; Howard, K. P. *Protein Sci.* **2005**, *14*, 856–861.
(41) Cady, S. D.; Hong, M. *Proc. Natl. Acad. Sci. U.S.A.* **2008**, *105*, 1483–1488.
(42) Hu, J.; Asbury, T.; Achuthan, S.; Li, C.; Bertram, R.; Quine, J. R.; Fu, R.; Cross, T. A. *Biophys. J.* **2007**, *92*, 4335–4343.
(43) Wang, J.; Kim, S.; Kovacs, F.; Cross, T. A. *Protein Sci.* **2001**, *10*, 2241–2250.

Table 1. Water-Accessible Surfaces and Pore Parameters of M2-TM in Viral Membranes Obtained from 3D Lattice Simulations of Water−Protein ^{1}H Spin Diffusion

Parameters	pH 4.5	pH 7.5	pH 7.5, Amt
Number of protein cubes	1592	1584	1608
Number of interface cubes	472	355	249
Number of drug cubes	0	0	28
V_P (nm^3)	12.7	12.7	12.8
S_{WP} (nm^2)	18.9	14.2	10.0
Relative S_{WP}	100%	75%	53%
S_{WP}/V_P	1.48	1.12	0.78
Minimum pore diameter (nm)	0.6	0.2	0

protein density of 1.43 g/cm^3.[44,45] These low-resolution models do not attempt to delineate the shape and volume of the side chains, but they are sufficient for determining the *change* of the protein−water surface area due to pH and drug binding. The center of the helical bundle was filled with water cubes, and one layer of interface cubes was used between the protein and water cubes. For the amantadine-bound state, the drug, whose approximate volume is 0.2 nm^3, was centered near Ser_{31} to be consistent with the recently determined high-resolution structure of the M2−amantadine complex[38] and with the observed maximal chemical shift perturbation at Ser 31.[27] The amide group of the drug was assumed to point down based on the recent crystal structure.[15]

The number of water cubes and protein−water interface cubes were varied to simulate the measured buildup curves, which were taken from the integrated intensities between 64 and 16 ppm in the ^{13}C DQ filtered spectra (Figure S2). Figure 5a shows the best-fit buildup curves for the three states. Side views of the structural models used to obtain the best fits are given in Figure 5b−d. The molecular distributions in all the planes across the bilayer are shown in Figures S6−S8. The low-pH sample exhibits the fastest buildup and was best fit by a protein−water surface area S_{WP} of 18.9 nm^2. Increasing the pH to 7.5 reduced S_{WP} by 25%, to 14.2 nm^2 (Table 1). Correspondingly, the minimum pore diameter was 0.6 nm (including the interface cubes) at pH 4.5 but decreased to 0.2 nm at pH 7.5. The requirement of keeping the protein volume constant while reducing the water-exposed area resulted in a tighter helical bundle with thicker cross sections at high pH (Figure 5c) and a more expanded helical bundle at low pH. This change, while simple, already reproduced certain features of MD simulations, such as the significantly reduced water amount in the vicinity of Val_{27} at high pH.[20,21]

Amantadine binding decreased S_{WP} further to 10.0 nm^2, representing a 47% reduction of the water accessibility compared to the low-pH state (Table 1). The channel is now devoid of water for approximately 6 planes or 12 Å along the pore axis (Figure S8). Thus the slow buildup of Gly_{34} and Ile_{35} is the direct result of amantadine-induced dehydration of the pore and the interruption of the water pathway between Val_{27} and Gly_{34}. It is worth noting that the spin diffusion experiment detects only *mobile* water sources and filters out the magnetization of potentially rigid water molecules. The crystal structure of M2-TM suggests that there may be rigid water molecules near Gly_{34},[15] which would not be detectable by the current technique.

In our simulations we assumed the water reservoir to be infinitely large, which was achieved by keeping the magnetization of each water cube at 100% throughout the spin diffusion process. Alternative simulations that allowed the water magnetization to decrease indicate that a water layer of ∼10 nm is necessary to reproduce the infinite-reservoir buildup behavior. The actual water amount in our samples corresponded to a water layer thickness of ∼4.5 nm for each lipid bilayer. This finite water reservoir may partly account for the drop of protein intensity at long mixing times. If a water amount approaching the 100% volume fraction (f_W) was used in the samples, then the equilibrium protein intensity $I_P(\infty)$ would be higher than observed, and normalization as required by eq 1 would reduce the initial slope, leading to a smaller water−protein surface S_{WP}. Expressed mathematically, the full equation for water−protein spin diffusion buildup includes dependence on both f_W and S_{WP} according to

$$\frac{I_P(t_m)}{I_P(\infty)} \approx \sqrt{\frac{D_{eff} t_m}{\pi}} \frac{1}{f_W} \frac{S_{WP}}{V_P} \tag{4}$$

Thus, when f_W is smaller than 1, the true S_{WP} is *smaller* than the apparent surface area $S'_{WP} = S_{WP}/f_W$ extracted from the buildup curves. Since the actual water amount in our samples is approximately 2-fold lower than the 100% limit, the 3D lattice calculations overestimate the true S_{WP} by 2-fold. On the other hand, the reduced complexity of the low-resolution 3D models compared to the true protein structure underestimates the actual S_{WP}. A recent study comparing S_{WP} obtained from spin diffusion data and from the VADAR web server[46] found that the spin diffusion analysis underestimates the water−protein surface area by approximately 3-fold.[25] Taken together, these two systematic errors should largely cancel to make the S_{WP} values in Table 1 quite realistic. Regardless of the absolute values of S_{WP}, the *relative changes* of the protein−water surface area are unaffected by these systematic uncertainties; thus the high-pH induced decrease of pore diameter and the drug-induced dehydration of the pore remain quantitatively valid.

Figure 6 shows a schematic of the water accessibility of the amantadine-bound M2 in lipid membranes, using the recently determined high-resolution structure of the drug-complexed M2-TM at high pH.[38] The virus-envelope-mimetic lipid bilayer is drawn to scale with the tetrameric helical bundle. Water from the two bilayer surfaces permeates to the top and bottom of the channel pore but is obstructed by the drug between Val_{27} and Gly_{34}. The amantadine location in the pore, obtained from independent protein−amantadine distance measurements,[38] is in excellent agreement with the observed reduction of the water-Gly_{34} spin diffusion rate in the drug-bound state.

Since the spin diffusion NMR technique probes water magnetization transfer on the long time scale of milliseconds, even in the somewhat confined environment between two membrane surfaces and within a channel, water would have diffused over hundreds of nanometers to micrometers and fully equilibrated with the protein protons if it is unobstructed. Thus, the fact that Gly_{34} in the middle of the helix showed significantly lower relative intensity at 4 ms than N-terminal residues indicates that the channel is blocked for milliseconds over many angstroms. This blockage time scale extends by 6 orders of magnitude the MD simulated nanosecond interruption of the

(44) Fischer, H.; Polikarpov, I.; Craievich, A. F. *Protein Sci.* **2004**, *13*, 2825–2828.
(45) Quillin, M. L.; Matthews, B. W. *Acta Crystallogr., Sect. D* **2000**, *56*, 791–794.
(46) Willard, L.; Ranjan, A.; Zhang, H.; Monzavi, H.; Boyko, R. F.; Sykes, B. D.; Wishart, D. S. *Nucleic Acids Res.* **2003**, *31*, 3316–3319.

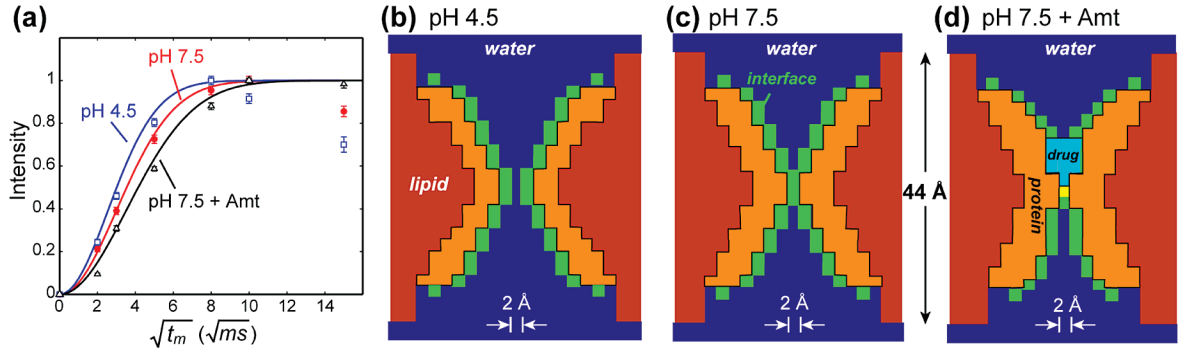

Figure 5. Quantification of the water-accessible surface area of M2-TM from ^{1}H spin diffusion buildup curves. (a) Normalized water-to-M2 spin diffusion buildup curves from the integrated intensities (64−16 ppm) of the 1D ^{13}C DQ filtered spectra. Error bars are 1−2% on the normalized scale and are mostly smaller than the symbols. Best-fit buildup curves (lines) were obtained as described in the text. (b−d) Low-resolution structural models of the M2-TM proton channels used to obtain the best fits. (b) pH 4.5. (c) pH 7.5. (d) pH 7.5 with bound amantadine. Water, blue; protein, orange; lipid, brown; water−protein interface, green; amantadine, cyan. The bilayer thickness (44 Å) and pixel size (2 Å) of the 3D lattice are indicated.

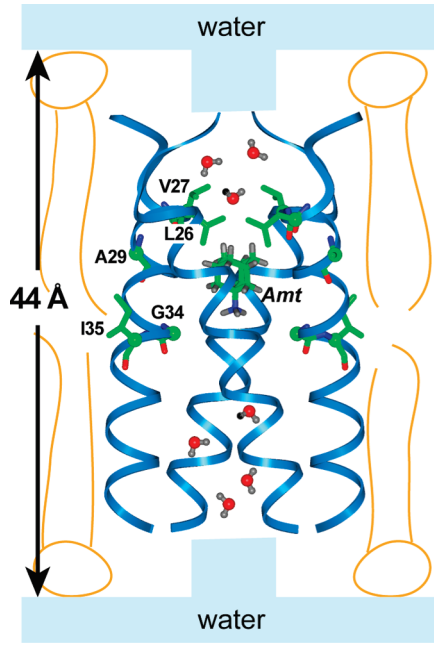

Figure 6. Water accessibility of amantadine-bound M2-TM at high pH in virus-envelope-mimetic lipid membranes. The water pathway through the pore is interrupted by amantadine. The five residues measured in this study are shown as sticks. The protein structure and amantadine position were determined from independent solid-state NMR distance experiments.[38] The bilayer thickness is shown to scale with the helical bundle. The water molecules in the channel are for illustration only; their density, orientation, and diffusion rate are outside the scope of this study.

water wire[19,20] and underscores the striking ability of amantadine to dehydrate the channel.

Conclusions

Using a ^{1}H spin diffusion NMR technique, we obtained for the first time experimental evidence of the pH- and drug-induced changes of the water accessibilities of the influenza M2 proton channel. At short mixing times, water-to-protein spin diffusion is primarily dependent on the radial position of the residues from the pore: lipid-facing residues receive less magnetization from water than pore-lining residues. Analysis of the integrated water−protein magnetization transfer indicates that the water-M2 surface area decreased by ∼25% from the open state to the closed state. This change is smaller than that of the chimeric potassium channel KcsA-Kv1.3, whose S_{WP} decreased by ∼40% from the open to the closed state.[25] Thus, the conformational changes associated with M2 channel activation are more modest, which is consistent with the fact that all key functions of this channel, including the selectivity filter and gating, are contained within a single TM helix, in contrast to multispanning potassium channels. Amantadine binding decreased the water accessibility of M2 by 47% compared to the open state, indicating that amantadine binds to the pore rather than the surface as suggested by a recent solution NMR study of M2(18−60).[18] The significant slowing-down of spin diffusion to Gly_{34} and Ile_{35} can only be explained by drug occlusion of the pore between Val_{27} and Gly_{34}, which interrupts the water pathway for several milliseconds. These results are in excellent agreement with the high-resolution structure of the amantadine-complexed M2 in lipid bilayers at high pH.[38] This spin diffusion NMR approach is generally applicable to membrane proteins and allows for the investigation of site-specific water−protein interactions and functionally important changes in the water accessibility and conformations of membrane proteins in lipid bilayers.

Acknowledgment. This work is supported by NSF Grant MCB-0543473 and NIH Grant R01 GM088204 to M.H. The 600 MHz solid-state NMR instrument was funded by an NSF grant and DBI-0421374. The authors thank Prof. Klaus Schmidt-Rohr for helpful discussions and Fanghao Hu for experimental assistance.

Supporting Information Available: Full 2D ^{1}H−^{13}C and ^{1}H−^{31}P spin diffusion spectra with complete assignment, 1D series of ^{13}C DQ filtered spin diffusion spectra, t_m^s extraction and table, water−lipid spin diffusion curves, and cube distributions for the 3D lattice simulations of spin diffusion are provided. This material is available free of charge via the Internet at http://pubs.acs.org.

JA9096219

Supplementary Information

Conformational Changes of an Ion Channel Detected Through Water-Protein Interactions Using Solid-State NMR Spectroscopy

Wenbin Luo and Mei Hong

Department of Chemistry, Iowa State University, Ames, IA 50011

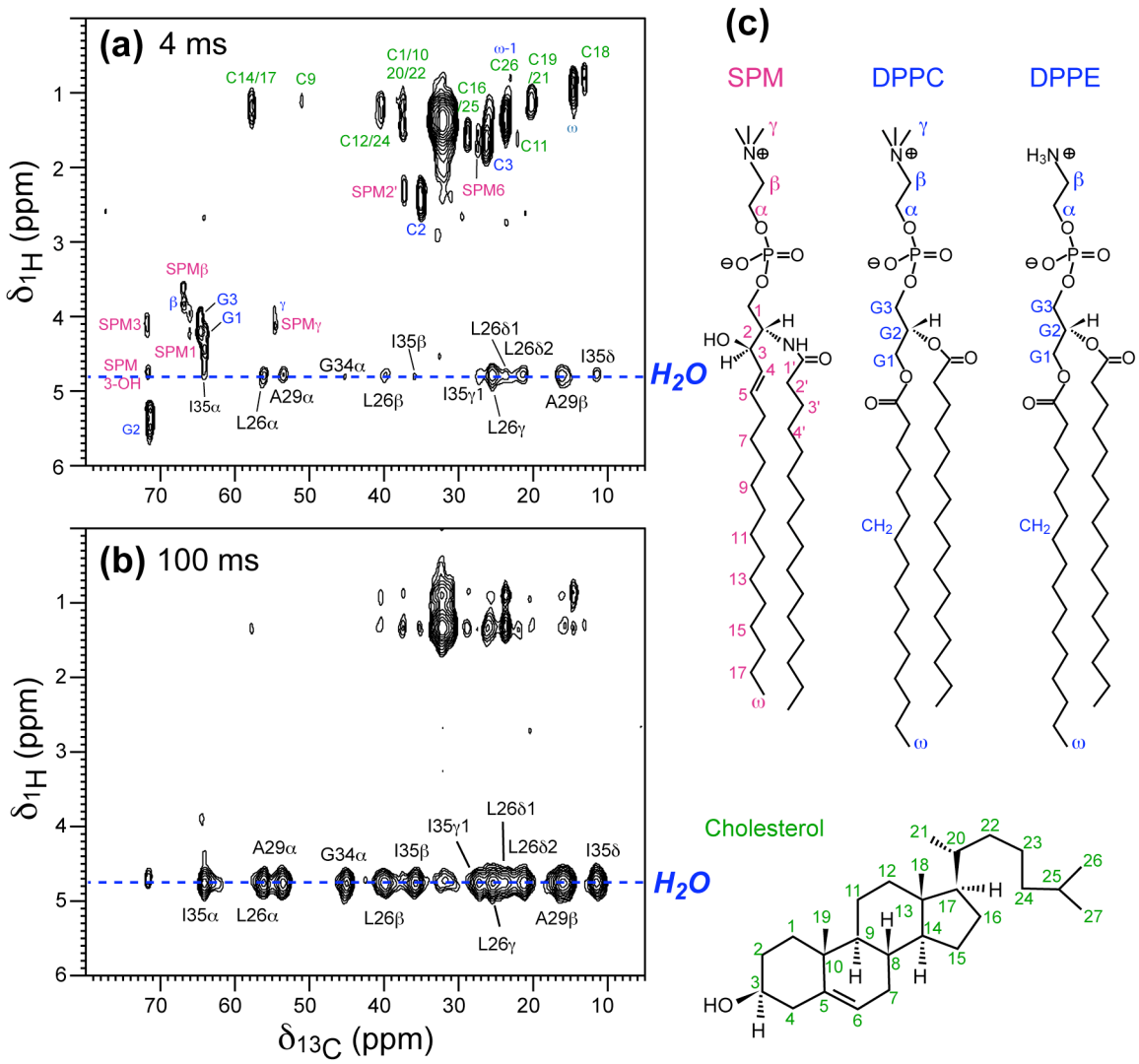

Fig. S1. Representative full 2D ^{13}C-^{1}H spin diffusion correlation spectra of M2-TM in viral membranes. The sample is the amantadine-bound M2-TM at pH 7.5. The spectra were measured at 293 K under 5 kHz MAS using a ^{1}H T_2 filter of 2 ms and varying spin diffusion mixing times. (a) 4 ms mixing. (b) 100 ms mixing. Intermolecular water-protein cross peaks are assigned in black. Intramolecular lipid and cholesterol ^{1}H-^{13}C cross peaks are also assigned. Cholesterol: green. Phospholipids: blue. Sphingomyelin (SPM): magenta.

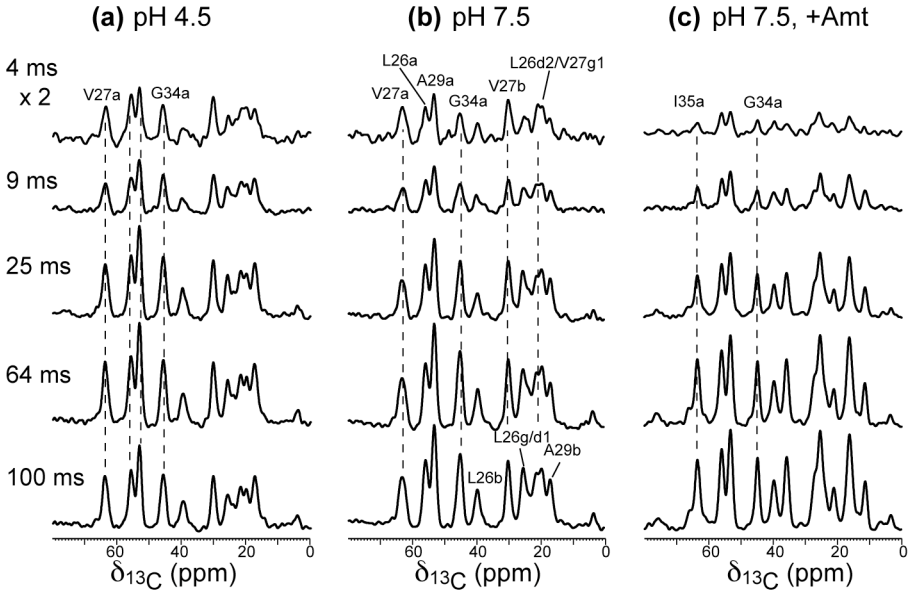

Fig. S2. ^{13}C DQ filtered spectra of M2-TM in viral membranes after ^{1}H spin diffusion from water. All spectra were measured using a ^{1}H T_2 filter of 2 ms at 293 K under 5 kHz MAS. Spin diffusion mixing times are indicated on the left. (a) pH 4.5. (b) pH 7.5. (c) pH 7.5 with amantadine. The spectra were plotted to scale within each sample. ^{1}H spin diffusion from water to Gly_{34} is slower than to N-terminal residues in the amantadine-bound sample, but is comparable in the two apo samples. Thus, in the absence of drug, both the low and high pH pores contain significant amount of water, while amantadine interrupts the water pathway between Ala_{29} and Gly_{34}. In the two apo samples, water-Ala_{29} spin diffusion is slightly slower than water-Val_{27} and water-Leu_{26} spin diffusion, consistent with the lipid-facing position of Ala_{29}.

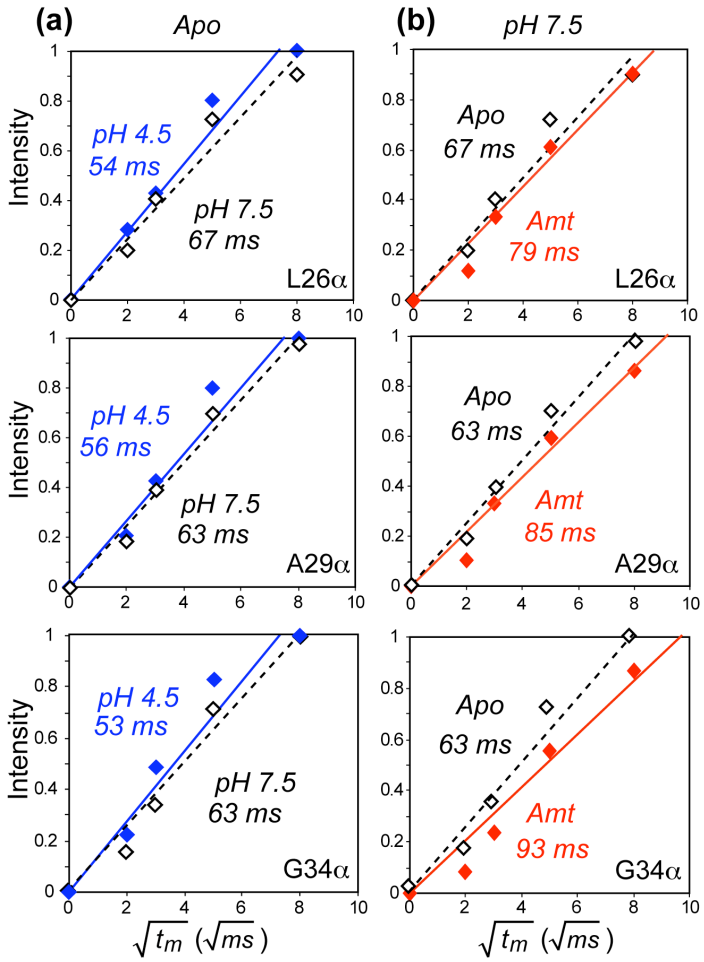

Fig. S3. Linear fitting of the initial rates of the water-to-M2 ^{1}H spin diffusion buildup curves to extract t_m^s values. Intensities are obtained from the 1D ^{13}C DQ filtered spectra (**Fig. S2**). (a) Comparison of the pH 4.5 (blue) and pH 7.5 (black) data without amantadine. (b) Comparison of the apo pH 7.5 data (black) and the amantadine-bound pH 7.5 data (red). For all labeled sites, the amantadine-bound protein at pH 7.5 has the longest t_m^s values, indicating that it has the lowest water accessibility, while the apo M2 at pH 4.5 has the shortest t_m^s values, indicating that the open state has the highest water accessibility.

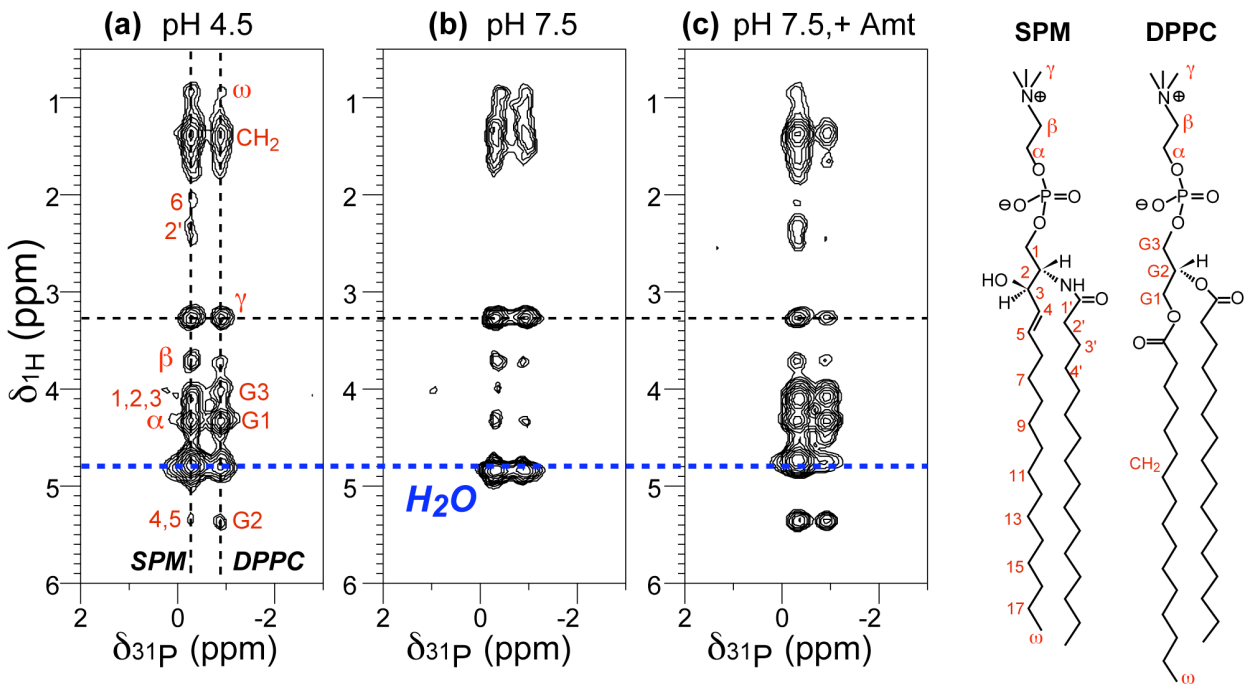

Fig. S4. 2D ^{1}H-^{31}P correlation spectra of membrane-bound M2-TM after ^{1}H spin diffusion. The spectra were measured with a ^{1}H T_2 filter of 0.8 ms and a spin diffusion mixing time of 64 ms at 293 K under 7 kHz MAS. (a) pH 4.5. (b) pH 7.5. (c) pH 7.5 with amantadine. Peak assignment is given in (a) along with the chemical structure and nomenclature of sphingomyelin (SPM) and DPPC on the right. The lipid Hγ signal is calibrated to be 3.26 ppm in each spectrum.

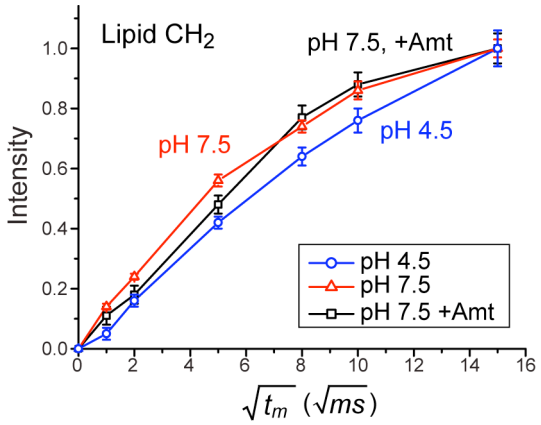

Fig. S5. Water-to-lipid spin diffusion for M2-containing viral membranes. Single-quantum ^{13}C spectra were measured with a ^{1}H T_2 filter time of 2.2 ms and varying spin diffusion mixing times at 293 K under 5 kHz MAS. The complete suppression of the initial lipid ^{1}H magnetization by the T_2 filter was confirmed by null intensity of the lipid CH_2 peak when the mixing time was set to 0. The low-pH membrane shows the slowest water-lipid spin diffusion, while the two high-pH samples have similar buildup rates with or without amantadine. This trend is different from and partly opposite to the water-protein spin diffusion behavior, indicating that the water-protein spin diffusion changes uniquely result from water accessibility changes of the protein, not from diffusion rate changes of water or lipids.

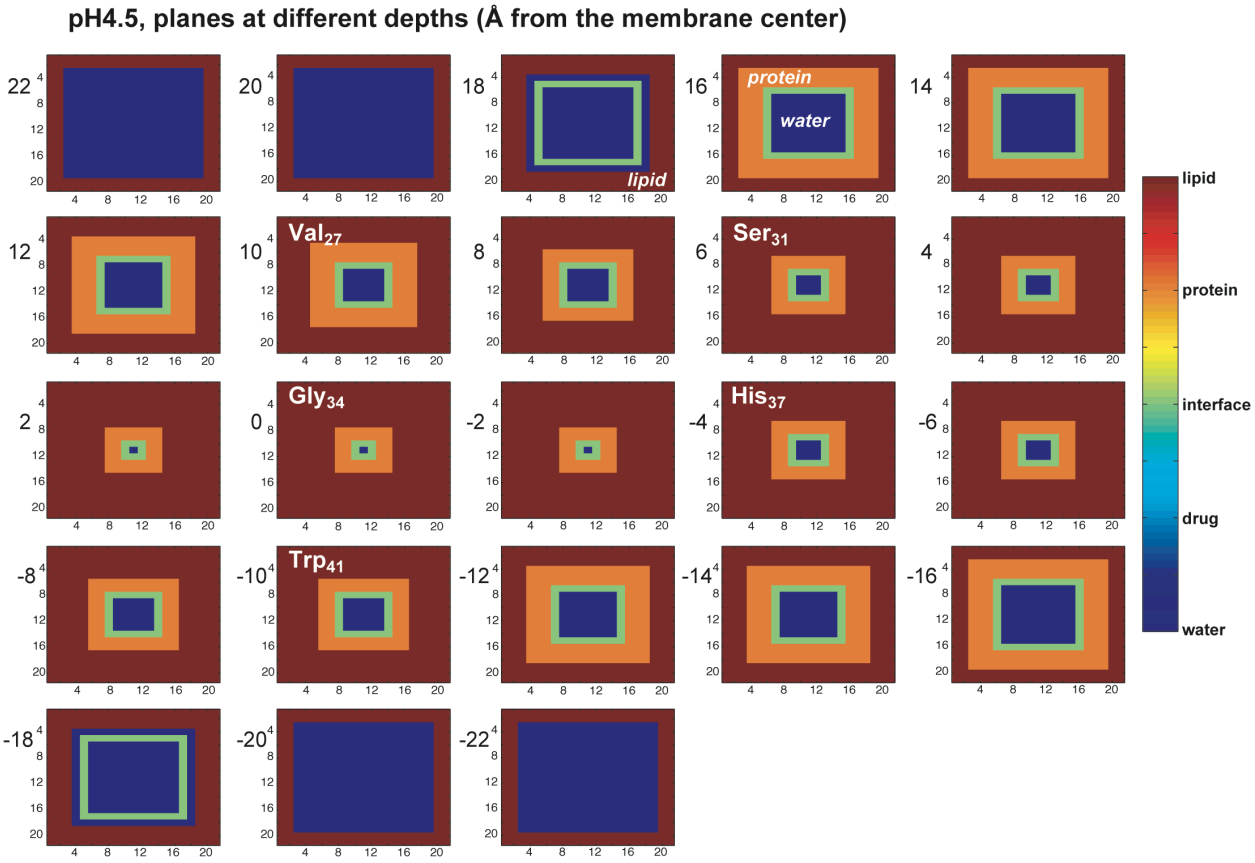

Fig. S6. Three-dimensional lattice used in the best-fit simulation of the water-to-protein spin diffusion buildup curve of M2-TM at pH 4.5. The spatial distributions of the water (dark blue), protein (orange), water-protein interface (green), and lipid (brown) cubes are shown for 23 planes spaced at 2 Å intervals along the bilayer normal. Approximate z-positions of key pore-lining residues on the lattice are indicated at appropriate planes.

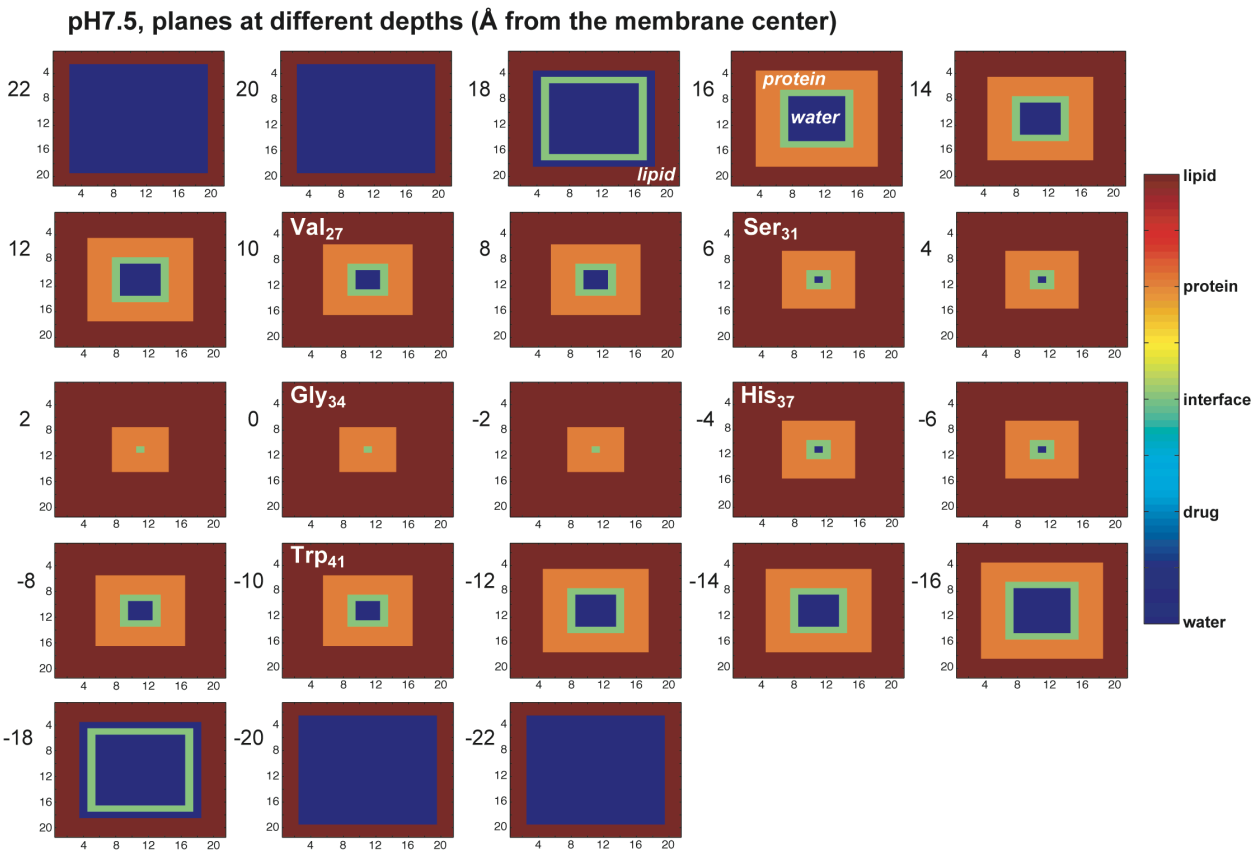

Fig. S7. Three-dimensional lattice used in the best-fit simulation of the water-to-protein spin diffusion buildup curve of M2-TM at pH 7.5 without amantadine. The spatial distributions of the water (dark blue), protein (orange), water-protein interface (green), and lipid (brown) cubes are shown for 23 planes spaced at 2 Å intervals along the bilayer normal. Approximate z-positions of key pore-lining residues on the lattice are indicated.

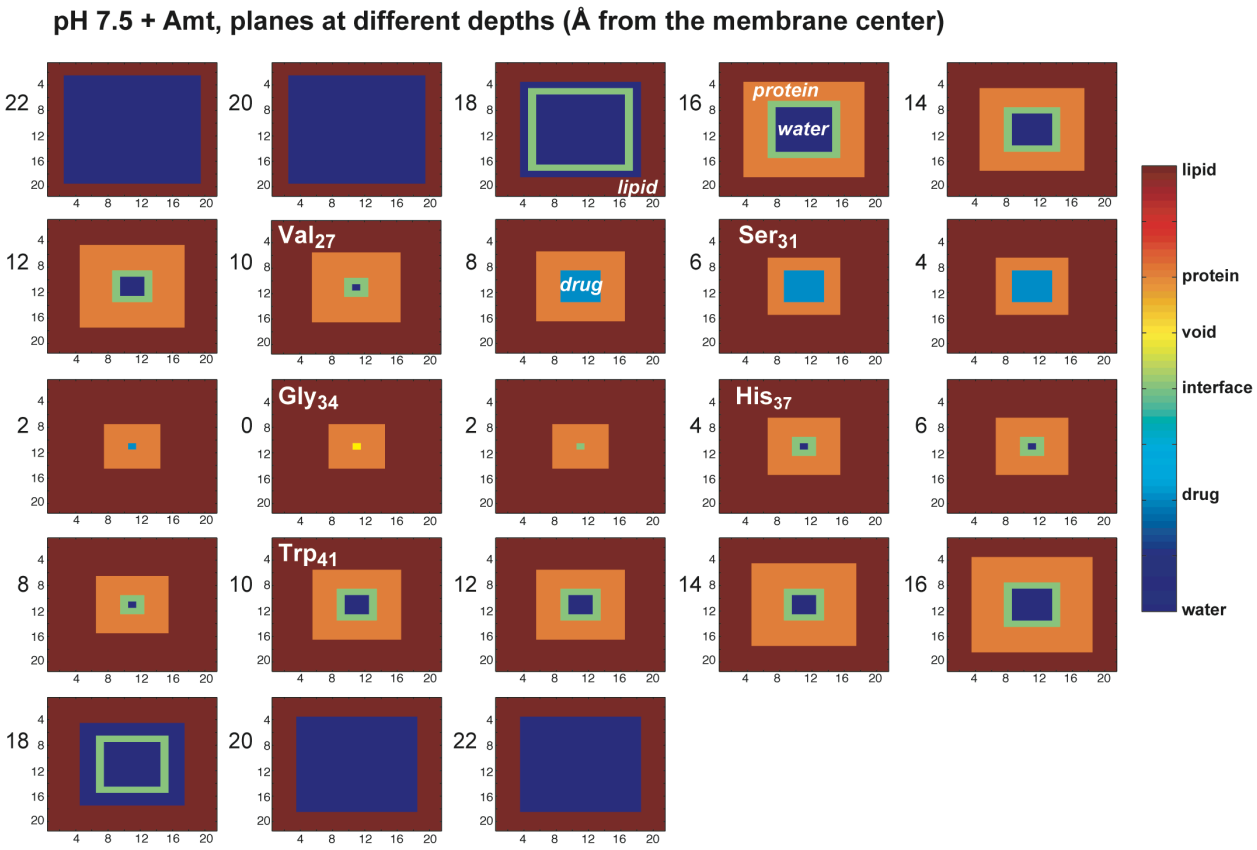

Fig. S8. Three-dimensional lattice used in the best-fit simulation of the water-to-protein spin diffusion buildup curve of amantadine-bound M2-TM at pH 7.5. The spatial distributions of water (dark blue), protein (orange), water-protein interface (green), amantadine (cyan), and lipid (brown) cubes are shown for 23 planes spaced at 2 Å intervals along the bilayer normal. Approximate z-positions of key pore-lining residues on the lattice are indicated. Note the exact z-position of the drug is qualitative and is not precisely determined from the current experiments.

Table S1. t_m^s values (ms) from the initial buildup rates of the ^{13}C DQ filtered ^{1}H spin diffusion spectra of M2-TM under different conditions.

Site	pH 4.5	pH 7.5	pH 7.5 + Amt
L26α	54±5	67±7	79±8
L26β	57±4	69±8	83±8
L26γ	53±7	68±8	82±9
L26 δ1	55±6	68±8	85±9
L26δ2/V27γ1	56±5	66±5	-
V27α	59±6	66±6	-
V27β	57±6	56±6	-
V27γ2	52±6	57±5	-
A29α	56±6	63±5	85±9
A29β	55±6	68±10	84±10
G34α	53±7	63±6	93±12
I35α	-	-	87±11
I35β	-	-	91±13
I35δ	-	-	88±11
Mean	55 ± 6	66 ± 7	86 ± 10